Cytometry PART A
ISAC Journal of Quantitative Cell Science

Centrifugation Affects the Purity of Liquid Biopsy-Based Tumor Biomarkers

Linda G. Rikkert,[1,2,3*] Edwin van der Pol,[3,4] Ton G. van Leeuwen,[3,4] Rienk Nieuwland,[2,3] Frank A.W. Coumans[2,3]

[1]Medical Cell BioPhysics, University of Twente, Enschede, the Netherlands

[2]Amsterdam UMC, University of Amsterdam, Laboratory of Experimental Clinical Chemistry, Amsterdam, the Netherlands

[3]Amsterdam UMC, University of Amsterdam, Vesicle Observation Center, Amsterdam, the Netherlands

[4]Amsterdam UMC, University of Amsterdam, Biomedical Engineering and Physics, Amsterdam, the Netherlands

Received 27 July 2018; Revised 28 September 2018; Accepted 1 October 2018

Grant sponsor: Netherlands Organisation for Scientific Research—Domain Applied and Engineering Sciences (NWO-TTW), Grant numberVENI 15924, Grant numberPerspectief CANCER-ID 14198, Grant numberVENI 13681

Additional Supporting Information may be found in the online version of this article.

*Correspondence to: Linda G. Rikkert; Amsterdam UMC, University of Amsterdam, Laboratory of Experimental Clinical Chemistry, Meibergdreef 9, Amsterdam 1105 AZ, the Netherlands. Email: l.g.rikkert@amc.uva.nl

Published online in Wiley Online Library (wileyonlinelibrary.com)

DOI: 10.1002/cyto.a.23641

Abstract

Biomarkers in the blood of cancer patients include circulating tumor cells (CTCs), tumor-educated platelets (TEPs), tumor-derived extracellular vesicles (tdEVs), EV-associated miRNA (EV-miRNA), and circulating cell-free DNA (ccfDNA). Because the size and density of biomarkers differ, blood is centrifuged to isolate or concentrate the biomarker of interest. Here, we applied a model to estimate the effect of centrifugation on the purity of a biomarker according to published protocols. The model is based on the Stokes equation and was validated using polystyrene beads in buffer and plasma. Next, the model was applied to predict the biomarker behavior during centrifugation. The result was expressed as the recovery of CTCs, TEPs, tdEVs in three size ranges (1–8, 0.2–1, and 0.05–0.2 μm), EV-miRNA, and ccfDNA. Bead recovery was predicted with errors <18%. Most notable cofounders are the 22% contamination of 1–8 μm tdEVs for TEPs and the 8–82% contamination of <1 μm tdEVs for ccfDNA. A Stokes model can predict biomarker behavior in blood. None of the evaluated protocols produces a pure biomarker. Thus, care should be taken in the interpretation of obtained results, as, for example, results from TEPs may originate from co-isolated large tdEVs and ccfDNA may originate from DNA enclosed in <1 μm tdEVs. © 2018 The Authors. Cytometry Part A published by Wiley Periodicals, Inc. on behalf of International Society for Advancement of Cytometry.

Key terms

biomarker; centrifugation; circulating cell-free DNA; circulating tumor cells; exosomes; extracellular vesicles; flow cytometry; microparticles; miRNA; tumor-educated platelets

Potential biomarkers in the blood of cancer patients include circulating tumor cells (CTCs) (1–3), tumor-educated platelets (TEPs) (4), tumor-derived extracellular vesicles (tdEVs) (5), EV-miRNAs (6), and circulating cell-free DNA (ccfDNA) (7,8). Typically, the first step to isolate a biomarker involves (differential) centrifugation, which isolates particles based on size and density. After centrifugation and optionally further processing, the biomarker is measured based on antigen exposure (CTCs and tdEVs) or on the composition of RNA (TEPs and EV-miRNAs) or DNA (ccfDNA). Fractions containing the biomarker of interest may be impure and contain substantial quantities of "contaminants", for example, other biomarkers. These contaminants may affect the obtained signal and potentially lead to the misinterpretation of results. Therefore, we applied a model based on the Stokes equation to assess the purity of biomarkers after centrifugation according to protocols used by other groups to study their biomarkers of interest (1–8).

Materials and Methods

Stokes Model

Figure 1 shows the principle of centrifugation. Before centrifugation, particles are uniformly distributed in a medium. Upon centrifugation, particles denser than the medium will travel toward the bottom of the tube. After centrifugation, the top

fraction is collected, defined here as the "supernatant." We define the "pellet" as the fraction remaining in the tube. The dashed line in Figure 1 is the interface between the supernatant and the pellet. The recovery of particles in the pellet is the fraction of particles in the pellet after centrifugation. This recovery depends on the starting point of the particle in the medium, as well as the densities and diameters of the particles. Consequently, the pellet will contain a high concentration of large and high density particles compared to the supernatant. For a swing-out rotor, the distance traveled by a particle can be modeled by the Stokes equation. In the Stokes equation, the speed of the particle results from the balance between the buoyant force and the drag force on a particle in a medium. In a centrifuge, the gravitational acceleration g depends on the distance from the axis of rotation.

$$g = R\omega^2 \tag{1}$$

where R is the distance to the axis of rotation and ω is the angular velocity of the centrifuge. After time T, the distance R of a particle starting at R_0 is given by the following equation:

$$R_T = R_0 e^{\frac{d^2(\rho_P - \rho_M)}{18\,S\,\eta}\omega^2 T} \tag{2}$$

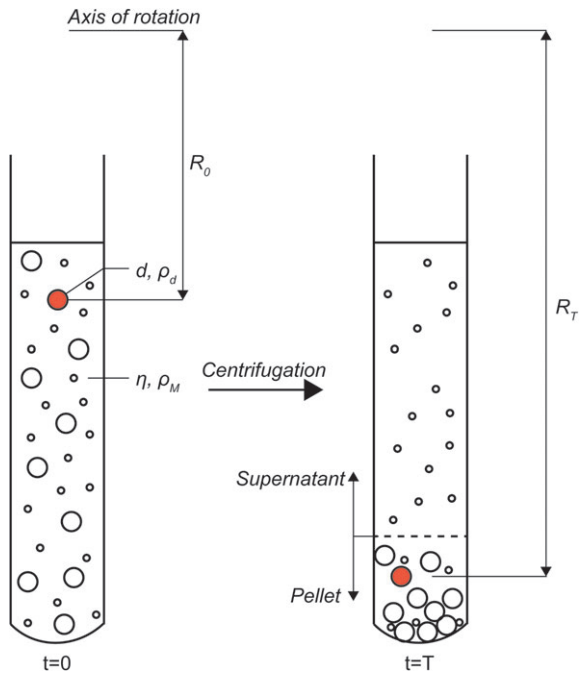

Figure 1. Centrifugation to isolate biomarker of interest from whole blood. The position of a particle after centrifugation can be described with the stokes equation (Eq. 2). Centrifugation of particles that are uniformly distributed throughout the sample causes large, high-density particles to move down to the pellet (below the dashed line), while small, low-density particles stay in the supernatant (above the dashed line). [Color figure can be viewed at wileyonlinelibrary.com]

where d and ρ_P are the diameter and the volumetric mass density of the particle and ρ_M and η are the volumetric mass density and viscosity of the medium. To allow nonspherical shapes such as platelets, the shape factor S is introduced (S = 1 for spheres). S accounts for the additional drag these nonspherical particles experience (9). Note that for nonspheres, d is the diameter of a sphere with equivalent volume. Model assumptions are (1) negligible wall effects, (2) instantaneous formation of the packed cell fraction during centrifugation of whole blood, and (3) aspiration sufficiently gentle not to disturb the pellet (see (10,11) for a complete description of the assumptions in the Stokes model). The model was programmed in Matlab (v2017a; MathWorks, Natick, MA) and applied to the evaluated centrifugation protocols.

Stokes Model Sample Properties

Table 1 shows the assumed sample properties, which were derived from the literature for a temperature of 20°C (see Supporting Information Table S1 for additional background). If available, volumetric mass densities were taken from references that applied density media with neutral osmotic effects. Platelets have a log-normal volume distribution (12) and a shape factor S of 2.0 (9,13). Platelets can have a volumetric mass density of 1.05–1.09 g/ml, where the lower density is associated with platelets that have secreted their α-granule content but with an unaffected platelet volume distribution (14,15). Most EVs have a diameter of <200 nm, which means that the volumetric mass density is substantially affected by the membrane density. A model describing EVs as cytoplasm enclosed by a cell-like membrane (16) leads to a size-dependent volumetric mass density. For EVs 100, 200, and 1,000 nm, the density is 1.099, 1.081, and 1.064 g/ml, respectively, which is in fair agreement with literature estimates between 1.08 and 1.11 g/ml (17–21). Finally, the mass density of ccfDNA is only available in cesium chloride media and the length of ccfDNA is unknown. Assuming a length of <1,000 base pairs, the ccfDNA would be smaller than 50 nm.

Model Validation

To validate the model, polystyrene beads were diluted in phosphate-buffered saline (PBS) or blood plasma. The concentration of beads was measured by flow cytometry before and after centrifugation at 300*g* for 20 min or 2,700*g* for 22 min using a Rotina 380R centrifuge (Hettich, Tuttlingen, Germany) or 15,800*g* for 60 min using a SW 41 Ti rotor and Optima L-80 XP ultracentrifuge (Beckman Coulter, Fullerton, CA), all at 20°C and with deceleration set to the minimum possible value. Polystyrene beads were 400, 799, 994, and 3,005 nm in diameter (Thermo Fisher Scientific, Waltham, MA) with a density of 1.05 g/ml. PBS (154 mM NaCl, 1.24 mM $Na_2HPO_4{\cdot}2H_2O$, 0.2 mM $NaH_2PO_4{\cdot}2H_2O$; pH 7.4) was 0.22 µm filtered (Merck, Darmstadt, Germany). Blood from anonymous healthy donors was obtained after written informed consent in accordance with the Dutch regulations and approved by the medical–ethical assessment committee of the Academic Medical Center, University of Amsterdam. Whole blood was drawn using a 21G needle in EDTA

Table 1. Stokes model sample properties

TYPE AND PROPERTY	VALUE USED IN MODEL	REFERENCES
CTCs		
Density (g/ml)	1.053	(24,25)
Diameter (μm)	Uniform. 8–20	(26)
Platelets		
Density (g/ml)	Norm., mean 1.069, SD 0.0053	(14,15,27)
Diameter (μm)	Lognorm., median 2.4, SD 0.6	(12,28)
Shape factor	2.0	(9,13)
EVs		
Density (g/ml)	Core 1.060, 8 nm shell 1.155	(17–21)
Diameter (μm)	Uniform. 0.05–1	
ccfDNA		
Density (g/ml)	1.7	(16,29)
Diameter (μm)	≤0.05	(16)
Polystyrene beads		
Density (g/ml)	1.05	MFG
Diameter (μm)		MFG
PBS		
Density (g/ml)	1.004	(30)
Viscosity (mPa s)	1.193	(30)
Plasma		
Density (g/ml)	1.0253	(31,32)
Viscosity (mPa s)	1.75	(33–35)

Values at 20°C (see Supporting Information Table S1 for more details). Lognorm., lognormal distribution; MFG, manufacturer specifications; Norm., normal distribution; SD, standard deviation; Uniform., uniform distribution.

vacutainers (BD Biosciences, San Jose, CA) and processed within 15 min after collection. Plasma was obtained from whole blood by double centrifugation at 2,500*g* for 15 min at 20°C using a Rotina 380R centrifuge. The supernatant was pooled between centrifugation steps and pooled before mixing with the polystyrene beads. The concentration of beads before and after centrifugation was measured on side scatter of a flow cytometer (FACSCalibur; BD, Franklin Lakes, NJ, 15 mW 488 nm laser, flow rate ~60 μl/min calibrated by weight (22), SSC 400 V, gain 0, threshold 0), and data were analyzed using FlowJo (v10; FlowJo LLC, Ashland, OR).

Predicted Performance of Centrifugation Protocols

We modeled the protocols as described in the literature and shown in Table 2. The dimensions of the low-speed centrifugation tube were derived from the 57.462 Sarstedt centrifugation tube and for ultracentrifugation from the 344059 Beckman Coulter centrifugation tube. For the model, we assume that centrifugation <10,000*g* is performed using a Rotina 380R centrifuge and centrifugation >10,000*g* using a SW41 Ti rotor and Optima L-80 XP ultracentrifuge. For most centrifuges, the set *g*-force is the force at the bottom of the tube. The force elsewhere is given by Eq. 1. This means that a

Table 2. Modeled centrifugation protocols

PROTOCOL	BLOOD VOLUME AND VACUTAINER	PROTOCOL SUMMARY	REFERENCES
CTCs/tdEVs	10 ml CellSearch	WB 7.5 ml:6.5 ml PBS 800*g*, 10 min → (10) Pel	(1–3,5)
TEPs	6 ml EDTA	WB 120*g*, 20 min → (3) Sup 360*g*, 20 min → (10) Pel, wash 2×	(4)
EV-miRNA	6 ml EDTA	WB 900*g*, 7 min → (5) Sup 2,500*g*, 10 min → (5) Sup 500*g*, 10 min → (5) Sup	(6)
ccfDNA (Speicher)	10 ml PAXgene ccfDNA	WB 200*g*, 10 min, 1,600*g*, 10 min → (3) Sup 1,600*g*, 10 min → (3) Sup	(8)
ccfDNA (Dawson)	10 ml EDTA	WB 820*g*, 10 min → (5) Sup 20,000*g*, 10 min → (10) Sup	(7)

ccfDNA, circulating cell-free DNA; CTCs, circulating tumor cells; EV-miRNAs, extracellular vesicle-associated miRNAs; TEPs, tumor-educated platelets; tdEVs, tumor-derived extracellular vesicles; WB, whole blood; → (*xx*) Pel, collect pellet *xx* mm above bottom of tube or buffy coat (for WB); → (*xx*) Sup, collect supernatant *xx* mm above bottom of tube or buffy coat (for WB).

10 cm high sample in a Rotina centrifuge set to 2,500*g*, has a *g*-force of 900*g* at the top of the sample. The same centrifugation protocol on a rotor with a larger diameter will increase the *g*-force at the top of the sample and thus result in an increased recovery in the pellet. However, we did not model multiple rotor diameters, because most rotors suitable for large tubes have diameters comparable to the Rotina 380R. Results are expressed as the % recovery of CTCs, TEPs, tdEVs in three size ranges from large (1–8 μm, "apoptotic bodies", "oncosomes", or "tumor microparticles"), intermediate (0.2–1 μm, "microparticles"), to small (0.05–0.2 μm, "exosomes") tdEVs, EV-miRNAs, and ccfDNA.

Results

Model Validation

Figure 2 shows the modeled and measured bead recovery in PBS (top) and plasma (bottom). As expected, the recovery of beads in the pellet increases with increased particle diameter, *g*-force, and centrifugation time. In addition, because plasma is more viscous than PBS, the recovery of beads in the pellet is lower in plasma compared to PBS. Modeled and measured recovery are in fair agreement (all errors <8%) for both PBS and plasma at 300*g* and 2,700*g*, as well as for PBS at 15,800*g*. The model overestimates the particle speed at 15,800*g* for plasma, with a maximum error of 20%. Thus, the model is a reasonable approximation to predict the behavior of spherical particles when applied to the centrifugation protocols as shown in Table 2.

Predicted Performance of Centrifugation Protocols

Table 3 shows the predicted recovery of number of particles based on the centrifugation protocols as shown in Table 2. The volume of the supernatant plus the volume of the pellet equals the starting volume. The volume reduction can be calculated by dividing the starting volume by the volume of supernatant or pellet. To obtain the particle concentration after centrifugation, the predicted recovery in the number of particles needs to be multiplied with the volume reduction, which is shown in the last column of Table 3.

The CTC protocol recovers 100% of CTCs but co-isolates substantial fractions of TEPs, large tdEVs, and ccfDNA. In subsequent epithelial cell adhesion molecule (EpCAM)-based magnetic enrichment of CTCs, the TEPs and ccfDNA will be removed, but tdEVs exposing EpCAM will be co-isolated. The latter is confirmed by a previous study, in which the CTC fraction was shown to contain large $EpCAM^+$ EVs (5).

The protocol to isolate TEPs predicts a yield of 71% together with 22% large tdEVs and <3% CTCs, smaller tdEVs, and ccfDNA. Because the subsequent processing includes detection of all mRNA present in the sample, our model indicates that additional evidence is needed to prove that the obtained RNA profiles indeed originate from platelets.

EV-miRNA samples contain intermediate tdEVs (40%), small tdEVs (57%), ccfDNA (57%), and TEPs and large tdEVs (<1%). By subsequent size exclusion chromatography (23), ccfDNA is removed, resulting in a relatively pure tdEV sample with high yield. The model predicts that the concentration of tdEVs is unaffected by the final centrifugation step

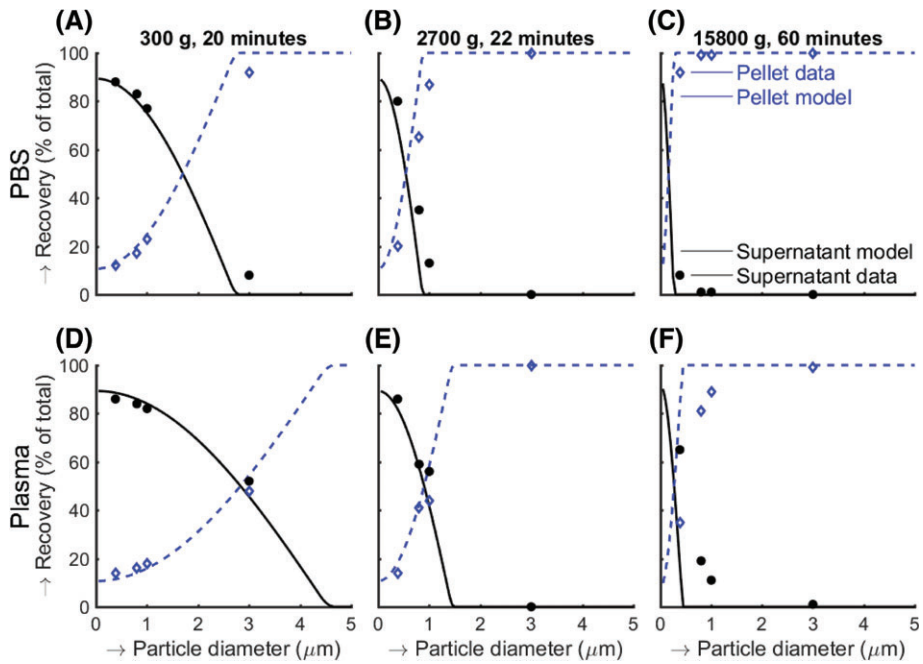

Figure 2. Centrifugation of beads diluted in PBS or plasma. The modeled bead recovery in pellet (blue dashed line) and supernatant (black, solid line) compared to measured bead recovery in pellet (open blue diamonds) and supernatant (closed black circles) for three centrifugation conditions. [Color figure can be viewed at wileyonlinelibrary.com]

Table 3. Predicted recovery (%) of centrifugation protocols

	CHANGE IN NUMBER (% OF ORIGINAL)						VOL. RED.
PROTOCOL	CTCS	TEPS	LARGE TDEVS	INTERMEDIATE TDEVS	SMALL TDEVS	CCFDNA	(FOLD)
CTCs/tdEVs	**100.0**	39.4	**81.1**	16.7	13.3	13.3	2.9
TEPs	0.0	**71.1**	21.7	3.2	2.2	2.2	3.0
EV-miRNA	0.0	0.01	**0.7**	**39.7**	**57.0**	56.9	1.7
ccfDNA (Speicher)	0.0	0.05	2.4	63.4	82.0	**82.0**	1.2
ccfDNA (Dawson)	0.0	6.10^{-7}	0.0	6.0	49.0	**48.4**	1.7

ccfDNA, circulating cell-free DNA; CTCs, circulating tumor cells; EV-miRNAs, extracellular vesicle-associated miRNAs; TEPs, tumor-educated platelets; tdEVs, tumor-derived extracellular vesicles; Vol. red., volume reduction. Bold font highlights the target component.

of the protocol, which is confirmed by the authors upon inquiry (6).

For ccfDNA, two centrifugation protocols were evaluated. The Speicher protocol (8) predicts the 82% recovery of ccfDNA, together with large tdEVs (2%), intermediate tdEVs (63%), small tdEVs (82%), and negligible CTCs and TEPs. The Dawson protocol (7) yields 48% of ccfDNA, but with lower contamination of intermediate tdEVs (6%), small tdEVs (49%), and negligible CTCs, TEPs, and large tdEVs. Thus, both protocols do not yield pure ccfDNA. Because the volumetric mass density difference between DNA and plasma is at least ninefold higher than the density difference for EVs, it is difficult to separate DNA from small EVs. Consequently, a 35 nm DNA "particle" travels at the same speed as a 100 nm EV.

Discussion

Centrifugation can be described with a model based on the Stokes equation. The model illustrates that centrifugation is effective at recovering particles that can be pelleted but that additional methods are needed to obtain a pure fraction. Particles with similar sedimentation rates are always co-isolated during centrifugation. This is especially relevant for TEP and ccfDNA protocols, because the co-isolated tdEVs may have substantial impact on the outcome. This model offers a tool to (re)design centrifugation protocols and at a minimum to establish whether available candidate protocols differ sufficiently from each other to warrant comparison. The model includes a shape factor to account for the nonspherical shape of platelets. This shape factor was set to 2.0 based on literature but was not experimentally validated.

For technologies evaluating the presence of CTCs, such as the CellSearch system, whole blood is centrifuged at 800*g* for 10 min. For this application, the model predicts a 100% effective isolation of CTCs, in addition to a recovery of 81% of the large tdEVs and 39% of TEPs. However, because of the use of imaging to identify each particle, tdEVs and TEPs can be distinguished from CTCs, and thus, the co-isolation does not affect the determined CTC concentration. Nevertheless, a purer CTC sample may be obtained by adjusting the centrifugation protocol. To reduce the recovery of TEPs or intermediate size tdEVs, the *g*-force or centrifugation time should be reduced. Because of their size, ccfDNA or small tdEVs' recovery in the pellet is mainly reduced by a reduction of the collection height.

The model predicts that a single biomarker cannot be purified by centrifugation alone. Substantial fractions of co-isolated other biomarkers remain present in all evaluated protocols, which may affect the obtained results and interpretation thereof.

Acknowledgments

This work was supported by the Netherlands Organisation for Scientific Research—Domain Applied and Engineering Sciences (NWO-TTW), research programs VENI 13681 (FC), Perspectief CANCER-ID 14198 (LR), and VENI 15924 (EvdP).

Conflict of Interests

The authors declare that the research was carried out in the absence of any personal, professional, or financial relationship that could potentially be construed as a conflict of interest.

Literature Cited

1. Cristofanilli M, Budd GT, Ellis MJ, Stopeck A, Matera J, Miller MC, Reuben JM, Doyle GV, Allard WJ, Terstappen LWMM, et al. Circulating tumor cells, disease progression, and survival in metastatic breast cancer. N Engl J Med 2004;351:781–791.
2. de Bono JS, Scher HI, Montgomery RB, Parker C, Miller MC, Tissing H, Doyle GV, Terstappen LWWM, Pienta KJ, Raghavan D. Circulating tumor cells predict survival benefit from treatment in metastatic castration-resistant prostate cancer. Clin Cancer Res 2008;14:6302–6309.
3. Cohen SJ, Punt CJA, Iannotti N, Saidman BH, Sabbath KD, Gabrail NY, Picus J, Morse MA, Mitchell E, Miller MC, et al. Prognostic significance of circulating tumor cells in patients with metastatic colorectal cancer. Ann Oncol 2009;20:1223–1229.
4. Best MG, Sol N, Kooi I, Tannous J, Westerman BA, Rustenburg F, Schellen P, Verschueren H, Post E, Koster J, et al. RNA-Seq of tumor-educated platelets enables blood-based pan-cancer, multiclass, and molecular pathway cancer diagnostics. Cancer Cell 2015;28:666–676.
5. Coumans FAW, Doggen CJM, Attard G, de Bono JS, Terstappen LWMM. All circulating $Epcam^{+}Ck^{+}Cd45^{-}$ objects predict overall survival in castration-resistant prostate cancer. Ann Oncol 2010;21:1851–1857.
6. van Eijndhoven MAJ, Zijlstra JM, Groenewegen NJ, Drees EEE, van Niele S, Baglio SR, Koppers-Lalic D, van der Voorn H, Libregts SFWM, Wauben MHM, et al. Plasma vesicle Mirnas for therapy response monitoring in Hodgkin lymphoma patients. JCI Insight 2017;1:1–19.

7. Dawson S-J, Tsui DW, Murtaza M, Biggs H, Rueda OM, Chin SF, Dunning MJ, Gale D, Forshew T, Mahler-Araujo B, et al. Analysis of circulating tumor DNA to monitor metastatic breast cancer. N Engl J Med 2013;368:1199–1209.
8. Heidary M, Auer M, Ulz P, Heitzer E, Petru E, Gasch C, Riethdorf S, Mauermann O, Lafer I, Pristauz G, et al. The dynamic range of circulating tumor DNA in metastatic breast cancer. Breast Cancer Res 2014;16:421.
9. Leith D. Drag on nonspherical objects. Aerosol Sci Technol 1987;6:153–161.
10. Livshits MA, Khomyakova E, Evtushenko EG, Lazarev VN, Kulemin NA, Semina SE, Generozov EV, Govorun VM. Isolation of exosomes by differential centrifugation: Theoretical analysis of a commonly used protocol. Sci Rep 2015;5:17319.
11. Price CA. *Centrifugation in Density Gradients*. Cambridge, MA: Academic Press, 2014.
12. Paulus J-M. Platelet size in man. Blood 1975;46:321–336.
13. White JG. *Platelet Structure. Platelets*. London: Elsevier, 2007;p. 45–73.
14. van Oost BA, Timmermans A, Sixma JJ. Evidence that platelet density depends on the alpha-granule content in platelets. Blood 1984;63:482–485.
15. Corash L, Tan H, Gralnick HR. Heterogeneity of human whole blood platelet subpopulations. I. Relationship between buoyant density, cell volume, and ultrastructure. Blood 1977;49:71–87.
16. Milo R, Jorgensen P, Moran U, Weber G, Springer M. Bionumbers—The database of key numbers in molecular and cell biology. Nucleic Acids Res 2009;38: D750–D753.
17. Choi D-S, Choi D-Y, Hong B, Jang S, Kim D-K, Lee J, Kim YK, Pyo Kim K, Gho YS. Quantitative proteomics of extracellular vesicles derived from human primary and metastatic colorectal cancer cells. J Extracell Vesicles 2012;1:18704.
18. Ji H, Greening DW, Barnes TW, Lim JW, Tauro BJ, Rai A, Xu R, Adda C, Mathivanan S, Zhao W, et al. Proteome profiling of exosomes derived from human primary and metastatic colorectal cancer cells reveal differential expression of key metastatic factors and signal transduction components. Proteomics 2013;13: 1672–1686.
19. Baietti MF, Zhang Z, Mortier E, Melchior A, Degeest G, Geeraerts A, Ivarsson Y, Depoortere F, Coomans C, Vermeiren E, et al. Syndecan–Syntenin–ALIX regulates the biogenesis of exosomes. Nat Cell Biol 2012;14:677–685.
20. Choi DS, Park JO, Jang SC, Yoon YJ, Jung JW, Choi DY, Kim JW, Kang JS, Park J, Hwang D, et al. Proteomic analysis of microvesicles derived from human colorectal cancer ascites. Proteomics 2011;11:2745–2751.
21. Lee E-Y, Park K-S, Yoon YJ, Lee J, Moon H-G, Jang SC, Choi KH, Kim YK, Gho YS. Therapeutic effects of autologous tumor-derived nanovesicles on melanoma growth and metastasis. PLoS One 2012;7:e33330.
22. van der Pol E, Sturk A, van Leeuwen T, Nieuwland R, Coumans F, ISTH-SSC-VB Working group. Standardization of extracellular vesicle measurements by flow cytometry through vesicle diameter approximation. J Thromb Haemost 2018;16: 1236–1245.
23. Boing AN, van der Pol E, Grootemaat AE, Coumans FAW, Sturk A, Nieuwland R. Single step isolation of extracellular vesicles by size-exclusion chromatography. J Extracell Vesicles 2014;3:23430.
24. Bryan AK, Hecht VC, Shen W, Payer K, Grover WH, Manalis SR. Measuring single cell mass, volume, and density with dual suspended microchannel resonators. Lab Chip 2014;14:569–576.
25. Wolff DA, Pertoft H. Separation of Hela cells by colloidal silica density gradient centrifugation: I. Separation and partial synchrony of mitotic cells. J Cell Biol 1972; 55:579–585.
26. Coumans FAW, van Dalum G, Beck M, Terstappen LW. Filter characteristics influencing circulating tumor cell enrichment from whole blood. PLoS One 2013;8: e61770.
27. Chamberlain K, Penington D. Monoamine oxidase and other mitochondrial enzymes in density subpopulations of human platelets. Thromb Haemost 1988;59:29–33.
28. Roper PR, Johnston D, Austin J, Agarwal SS, Drewinko B. Profiles of platelet volume distributions in normal individuals and in patients with acute leukemia. Am J Clin Pathol 1977;68:449–457.
29. Mattoccia E, Comings DE. Buoyant density and satellite composition of DNA of mouse heterochromatin. Nat New Biol 1971;229:175–176.
30. Lide D. *CRC Handbook of Chemistry and Physics*. Boca Raton, FL: CRC Press, 2005.
31. Trudnowski RJ, Rico RC. Specific gravity of blood and plasma at 4 and 37°C. Clin Chem 1974;20:615–616.
32. Kenner T. The measurement of blood density and its meaning. Basic Res Cardiol 1989;84:111–124.
33. Késmárky G, Kenyeres P, Rábai M, Tóth K. Plasma viscosity: A forgotten variable. Clin Hemorheol Microcirc 2008;39:243–246.
34. Lawrence J. The plasma viscosity. J Clin Pathol 1950;3:332–344.
35. Hess EL, Cobure A. The intrinsic viscosity of mixed protein systems, including studies of plasma and serum. J Gen Physiol 1950;33:511–523.